Tomasz CHMIELEWSKI, Piotr ORAMUS, Tomasz KUCZEK

ABB sp. z o. o., Corporate Research Center, Kraków, Poland

Switching overvoltage analyses under distorted supply voltage conditions

Abstract. This paper presents the impact of the higher harmonics presence in the supply voltage on the generated transient recovery voltage (TRV), which inherently appear between circuit breaker contacts (CB) after current interruption. In the current version the international standards from committees such as CIGRE or IEC are silent about this topic. The research presented in this paper, includes laboratory experiments and simulations, for ideal supply voltage conditions and the supply voltage with certain harmonic content. The black-box conductance model of electric arc, based on Cassie-Mayr equation was used for the simulations.

Streszczenie. Artykuł przedstawia analizę wpływu wyższych harmonicznych w napięciu zasilającym na napięcie powrotne (TRV) pojawiające się między stykami wyłącznika po przerwaniu prądu. Motywacją do powstania artykułu stał się fakt, iż normy międzynawowych komitetów takich jak CIGRE czy IEC w obecnych wersjach nie poruszają tego zagadnienia. Artykuł zawiera wyniki analiz oraz eksperymentów laboratoryjnych dla warunków bez harmonicznych oraz z harmonicznymi obecnymi w napięciu zasilającym. W symulacjach zastosowano model łuku elektrycznego w oparciu o równania Cassiego – Mayra. Analiza wpływu wyższych harmonicznych w napięciu zasilającym na napięcie powrotne między stykami wyłącznika

Słowa kluczowe: koordynacja izolacji, napięcie powrotne, łuk elektryczny, Cassie-Mayr, wyższe harmoniczne, stany nieustalone
Keywords: insulation co-ordination, TRV, Cassie-Mayr, arc, harmonics, distortion, transients

1. Introduction

The insulation co-ordination analyses are the inevitable stage during the process of reliable electrical systems design. The general purpose of such analyses is most commonly to estimate the maximum (worst case scenario) values of possible overvoltages, for example in various transient states. The outcome of the insulation co-ordination study is crucial for verification of ratings of the power system equipment, as well as overall design of e.g. power substation. Computer simulations are nowadays considered to be an efficient and trustworthy tool that can be applied for analyses of transient conditions. What is more, there are numerous guidelines for computer modelling, which are provided by the international standardization committees and working groups [1-9]. According to IEC and IEEE standards, the substantial part of insulation co-ordination studies (at all voltage levels) is determination of switching transients, generated during current interruption or circuit energization operation [1-5]. As recommended by the IEC standard [1, 2], the determination of switching transients can be done using either deterministic or statistical method with uniform or standard Gaussian distribution of the opening time instant. One of the most valuable information that can be obtained during these studies is the Transient Recovery Voltage (TRV) appearing between Circuit Breaker (CB) contacts, after current interruption. The analysis of phenomena related to switching transients and harmonics (especially with a strong focus on simulations) has been widely investigated in literature [10-16].

In all of the herein quoted resources (papers and standards), the development of the model for transient simulation includes representation of utility grid that supplies the voltage to the system. This element may be represented in various ways, depending on the type of the analysis. Nonetheless, it is usually based on Thevenin equivalent circuit approach, which comprises ideal voltage source, coupled with certain combination of passive elements. The topic of network equivalent models has been elaborated in [1, 7, 8, 9, 17-20]. In general, it can be pointed out, that the network equivalent should provide a sufficient response (i.e. reflecting the actual network parameters) in a given frequency range [1]. Nonetheless, each of abovementioned models assumes the purely sinusoidal supply voltage. Nowadays, due to large number of nonlinear loads (e.g. power electronics converters operating in switch mode), the utility voltage often contains higher harmonics [21-23]. In fact, the relevant international standards provide maximum permissible levels for total and individual harmonics distortion in the supply voltage [24-26]. However, one should bear in mind that these levels may be even higher. For instance, if the given installation operates in islanded mode or if the considered node is not the point of common coupling with the grid, the voltage quality does not have to comply with the grid codes requirements. Furthermore, when it comes to very short-time effects (3 seconds or less) the requirements regarding individual harmonic content and the total harmonic distortion (THD) are less strict [25, 26]. As indicated in [25], these values may be even 1.5 times higher than in case of long term-effects (10 minutes or more). Hence, according to [25], the maximum short-term THD amounts to 12% for LV (1 kV and below) systems and 2.25 % for HV (161 kV and above) systems.

The main goal of this paper is to investigate to what extent, the presence of harmonics in source voltage affects the overvoltages generated during current interruption. For this reason, simulations of a high voltage (HV) and low voltage (LV) test systems were employed. The simulation results obtained for LV test system were additionally verified by means of laboratory experiments. Based on the obtained TRV and current traces, the relevance of including the harmonic spectrum during switching surge studies was evaluated.

2. Switching transients and harmonics in power systems

Transient overvoltages in power systems can be classified according to their magnitude, rise time and frequency spectrum. Overvoltages can be generated during various types of phenomena, both switching and lightning ones. International standards [1, 2] classifies transients into two categories: low frequency and high frequency. Low frequency transients are related to daily load variations, faults, load rejection as well as ferroresonance. Their magnitudes can reach values around 2.0 p.u. in range of frequency from 10 Hz to 500 Hz. Second class – high frequency transients – are related to three different sub-groups: fast-front, very-fast-front and slow-front transients. First one is related to lightning phenomena, occurring at

medium and HV overhead transmission lines. The Very-Fast-Front Transients (VFFT) can be caused by disconnector or CB operations within the Gas Insulated Switchgear (GIS) substations. Slow-front transients, which are the main concern of this paper, are related to energization and de-energization of transmission lines, transformers and shunt reactors. Herein, the emphasis is laid on breaking of inductive currents. Analysis of these events is very important from the point of view of insulation co-ordination for medium and HV substations (both air and SF$_6$ insulated). This is due to the chopping of current before its natural zero crossing, which can result in generation of severe overvoltages, emanating at the circuit that is de-energized (e.g. transformer or shunt reactor). Typical overvoltage trace that occurs at the inductive load upon CB opening is presented in Fig. 1.
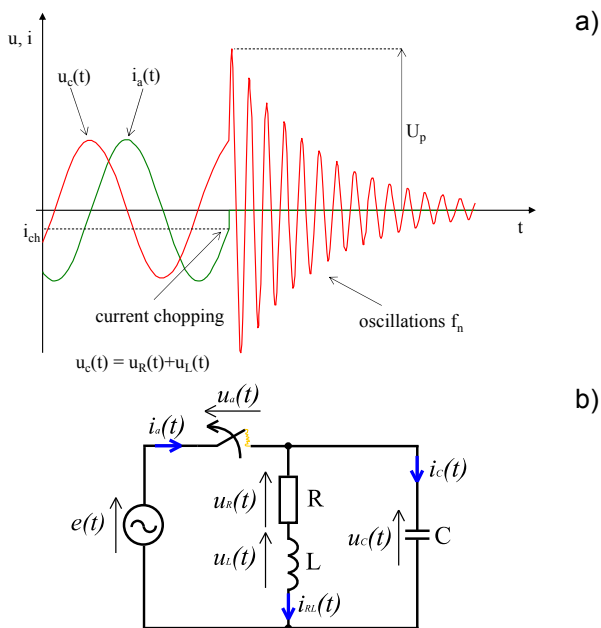
Fig. 1. Principle of inductive current breaking [28], [29]; i_{ch} – chopping current in A, I_N – nominal current peak in A, U_N – nominal phase voltage in V, U_p – peak voltage after de-energization in V, f_0 – frequency of oscillations in Hz

After physical separation of operated CB contacts current is conducted through the air until it subsides to the chopping current value i_{ch}. The energy that is trapped in de-energized compartment starts to oscillate between circuit's equivalent inductance and capacitance, according to (1) [28, 29]. Resulting overvoltage trace is characterized with frequency f_0 defined by (2) and maximum overvoltage peak value U_p calculated according to (3), neglecting resistive damping (Fig. 1b) [28, 29]. As can be observed frequency f_0 is independent of the source voltage.

$$(1) \qquad \frac{1}{2}Li_{ch}^2 = \frac{1}{2}CU_p^2$$

$$(2) \qquad f_0 = \frac{1}{2\pi\sqrt{LC}} \quad (2)$$

$$(3) \qquad U_p = \sqrt{\frac{L \cdot i_{ch}^2}{C}}$$

where: L – load inductance in H, C – load stray capacitance in F, U_p – maximum overvoltage peak value in V, i_{ch} – chopping current in A, f_0 – frequency of oscillations in Hz.

As far as the modelling of CB opening process is under consideration, there are two methods recommended by the IEC standard [1, 2]. The simplest approach is to utilize the ideal interrupter with predefined value of i_{ch}. It represents a very high resistance at open state and very low resistance when closed. The level of the chopping current can be evaluated according to (4) [30]:

$$(4) \qquad i_{ch} = \lambda \cdot C_p^a \cdot N^b$$

where: N – number of breaking chambers, C_p – "effective" parallel capacitance seen from circuit breaker terminals in F, λ – chopping number in A·F$^{-0.5}$, a, b – equation constants often assumed to be equal 0.5.

The ideal electrical AC power network should supply perfectly sinusoidal, symmetrical voltage at the desired frequency. Unfortunately, mainly due to presence of nonlinear loads and switch-mode power electronic devices often the voltage contains also higher component harmonics. Sources of harmonics emission are outlined in [27]. Such distorted periodic waveform can be represented as algebraic sum of fundamental component and harmonics (17):

$$(5) \qquad U(t) = U_0 + \sum_{k=1}^{\infty} h_k \sin(k \cdot \omega \cdot t + \Psi_k)$$

where: k – harmonic order (k = 1 is the fundamental component, U_0 – possible offset in V, h_k – peak value of k harmonic component, ω – rated angular frequency in rad/s, t – time in s, ψ_k – phase angle of n harmonic component at t = 0 expressed in rad.

As can be noticed in (5) each component is characterized by its amplitude and phase. Both of these parameters affect the shape of periodic signal. However, harmonics phase is often neglected in the power quality studies due to the fact that international standards provide maximum limits only on the amplitude of individual harmonics and resulting quality indicators such as total harmonic distortion (THD), which is independent of individual components phase [25, 28].

4. Circuit breaker black-box models for switching analyses

Another way of CB modelling proposed by [1] is a so-called Cassie-Mayr non-linear conductance black-box model. This model accounts for complex process of electric arc forming between CB contacts, during its opening phase. The Cassie electric arc behavior is described by the following equation:

$$(6) \qquad \frac{dg_c}{dt} = \frac{1}{\tau_c} \cdot \left(\frac{i_a \cdot u_a}{U_s^2} - g_c \right)$$

where: where: g_c – arc conductance calculated according to Cassie equation in S, τ_c – Cassie time constant of the arc in s, P_0 – steady-state power loss of the arc in W, U_s – stationary arc voltage in V, u_a – arc voltage in V, i_a – arc current in A.

The Mayr equation is given by (7) [31]:

$$(7) \qquad \frac{1}{g_m} \cdot \frac{dg_m}{dt} = \frac{1}{\tau_m} \cdot \left(\frac{u_a \cdot i_a}{P_0} - 1 \right)$$

where: g_m – the arc conductance calculated according to Mayr equation in S, τ_m – the Mayr time constant of the arc in s, P_0 – the steady-state cooling power of the arc in W, i_a – arc current in A, u_a – arc voltage in V.

In general, the Mayr portion represents electric arc behavior for low currents, whereas Cassie portion for high currents, hence their parameters are tuned individually for each equation. The CB is considered open, as soon as the resulting arc resistance reaches 108 Ω [1]. Thus, the Cassie-Mayr black-box model is essentially a connection of two models: Mayr model and Cassie model. Therefore, the total arc resistance is given by (8) [32]:

$$(8) \qquad r_{arc} = \frac{1}{g_{arc}} = \left(\frac{1}{g_c} + \frac{1}{g_m} \right)$$

where: g_c – the arc conductance calculated according to the Cassie portion (5) in S, g_m – the arc conductance calculated according to the Mayr portion (7) in S.

The mathematical derivation of supply voltage impact on the current breaking is presented based on Mayr equation and RLC circuit depicted in Fig. 1b (the same routine can be used for Cassie portion). The Mayr equation (7) can be transformed as follows:

$$(9) \qquad \frac{1}{g_m} \cdot \frac{dg_m}{dt} = \frac{1}{\tau_m} \cdot \left(\frac{i_a \cdot u_a}{P_0} - 1 \right)$$

$$(10) \qquad \int \left(\frac{1}{g_m} \right) dg_m = \frac{1}{\tau_m} \cdot \int \left(\frac{i_a \cdot u_a}{P_0} - 1 \right) dt$$

$$(11) \qquad \ln g_m + \ln \left(\frac{1}{g_0} \right) = \frac{1}{\tau_m} \cdot \int \left(\frac{i_a \cdot u_a}{P_0} - 1 \right) dt$$

$$(12) \qquad \ln \left(\frac{g_m}{g_0} \right) = \frac{1}{\tau_m} \cdot \int \left(\frac{i_a \cdot u_a}{P_0} - 1 \right) dt$$

$$(13) \qquad \frac{g_m}{g_0} = e^{\frac{1}{\tau_m} \int \left(\frac{i_a \cdot u_a}{P_0} - 1 \right) dt} \quad / \cdot g_0$$

Thus, the final solution of equation (8) can be described as:

$$(14) \qquad g_m = g_0 \cdot e^{\frac{1}{\tau_m} \int \left(\frac{i_a \cdot u_a}{P_0} - 1 \right) dt}$$

For circuit illustrated in Fig.1, the following set of equation is met:

$$(15) \qquad \begin{cases} e(t) = U_0 + \sum_{k=1}^{\infty} h_k \sin(k \cdot \omega \cdot t + \Psi_k) \\ e(t) = u_a(t) + u_C(t) \\ e(t) = u_a(t) + u_L(t) + u_R(t) \\ i_a(t) = i_{RL}(t) + i_C(t) \end{cases}$$

where: k – harmonic order ($k = 1$ is the fundamental component), U_0 – possible voltage offset in V, h_k – peak value of k harmonic component, ω – rated angular frequency in rad/s, t – time in s, ψ_k – phase angle of k harmonic component at $t = 0$ expressed in rad.

Thus, combining set of equations (15) with final solution of Mayr equation (14), the time-dependent arc conductance g(t) formula can be expressed in the following way:

$$(16) \qquad g(t) = g_0 \cdot e^{\frac{1}{\tau_M} \int \left(\frac{\left(U_0 + \sum_{k=1}^{\infty} h_k \sin(k \cdot \omega \cdot t + \Psi_k) - u_C(t) \right) \cdot i_a(t)}{P_0} - 1 \right) dt}$$

where: g_0 – arc conductance in previous time step in S.

Equation (16) shows direct influence of source voltage harmonics content on arc conductance during current

interruption process, what in consequence has impact on TRV character.

5. Study cases

In the course of performed analysis, two basic scenarios have been distinguished for all configurations under study. First one assumes purely sinusoidal power supply, whereas in case of second one, the voltage with a specific harmonic spectrum was applied. In case of both supply voltage types (i.e. with and without harmonics) the amplitude, phase and frequency of the fundamental voltage component are identical. These two types of power supply were subsequently applied for two test circuits described in details in sections 6.1 and 7.1. Simulations and experiments outcomes are current and TRV traces occurring between the interrupter contacts. In each simulation and experimental case study, only the current interruption was considered (i.e. opening operation). The HV circuit described in section 6.1 was analyzed only using the EMTP-ATP simulations, whereas the LV system presented in section 7.1 was verified both experimentally and by means of simulations. Additionally, an investigation for individual harmonics impact was carried out. It was assumed during this investigation, that only single harmonic is present at the supply source. The results were extracted individually for harmonics in range from 2nd to 50th. Two parameters were selected as decisive when evaluating the impact of the harmonics in the supply voltage on the TRV and the entire interruption process. First one is the peak value of the TRV between the interrupter contacts (measured for both HV test circuit and laboratory setup). Second one is the arcing time (calculated only in case of LV test circuit), which is calculated from the instant when the interrupter opening starts, to the moment when the current drops to zero.

6. Circuit description and study cases

In order to initially verify the impact of non-ideal supply voltage on TRV, the first test was carried-out using only simulations conducted in EMTP-ATP software. For this purpose, a simplified three-phase 345 kV system, was developed for the simulation of inductive current breaking process. The test circuit comprised: linear shunt reactor (equivalent RLC load), 100 km line modelled as surge impedance and grid equivalent that included the positive and zero sequence short-circuit impedances. The long overhead line represented the network up to two buses away from the point of interest [8]. The CB was modelled as an ideal switch, with chopping current level assumed at 3 A. The diagram of HV system used for the simulation is presented in Fig. 2.
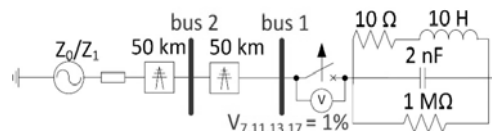
Fig. 2. Simplified 345 kV, 3-phase system for simulations only

Model parameters of considered power system are listed in Table 1.

Table 1. Components data of the simplified HV test system [8]

System component	Parameters
Overhead line	$\underline{Z}_1$ =(0.04+j0.318) Ω/km, $\underline{Z}_0$=(0.26+j1.015)Ω/km C_1 =11.86 nF/km, C_0 =7.66 nF/km
Network equivalent	$\underline{Z}_1 = \underline{Z}_0 = (6.75+j127)$ Ω U_{L-L} = 345 kV, f = 50 Hz
Circuit breaker	$I_{chopping}$ = 3 A

As illustrated in Fig. 2, at the point where the voltage measurement was performed, the 1% of 7th, 11th, 13th and 17th harmonics are present in the supply voltage (all harmonics are in phase with the fundamental component of the supply voltage). The selected harmonics can be considered typical in vicinity of HVDC terminal. As defined by [26], individual harmonics content in voltage for systems above 161 kV should be no more than 1% and resulting THD should be lower than 2%, hence assumed conditions comply with the guidelines outlined therein. Fig. 3 depicts both sinusoidal and contaminated voltage.
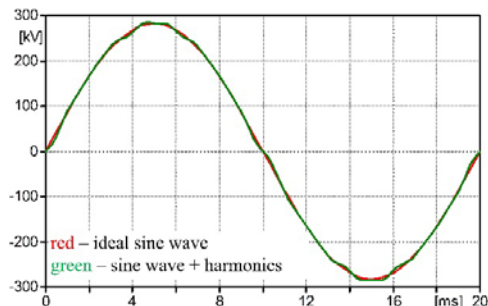
Fig. 3. Three phase supply voltage (only one phase is shown for better visibility) applied for simulation of HV test system

For better visibility only single-phase is shown. Two remaining phases are identical in shape and accordingly shifted by 120 degrees, forming a symmetrical three phase supply.

Such simplified approach was intended to facilitate the results interpretation. Therefore, only four most typical harmonics are present in the supply voltage. Moreover, in this case only the harmonics impact on TRV was investigated. It should be underlined that the HV system was chosen mainly due to numerous standardization committees modelling guidelines (including input data), which are easily accessible and most importantly – well established. Hence, the modelling approach is compliant with [1, 7, 8, 9].
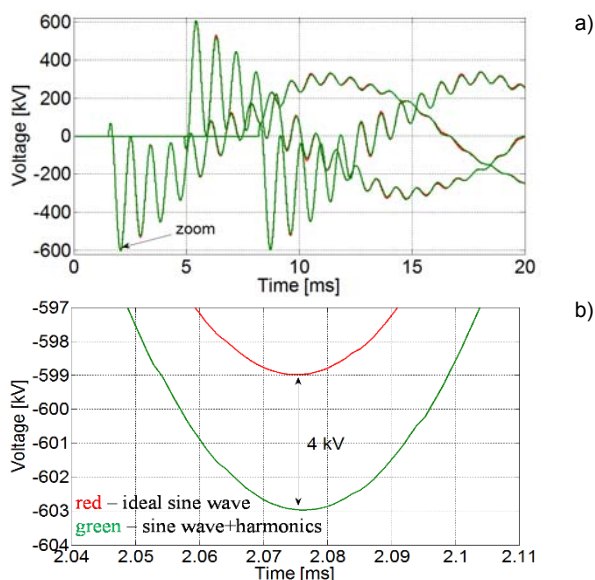
Fig. 4. Test circuit verified through simulations: (a) 3-phase TRV (single-phase view) for ideal supply voltage (red) and supply voltage with harmonics (green); (b) extended view on single phase (zoomed part is marked in (a))

6.2. HV test circuit

In this section, results obtained from the simulation of 345 kV three-phase test circuit are presented. The simulations were conducted on the circuit depicted in Fig 2. As explained above they were used to initially verify the impact (if any) of voltage harmonics on the generated TRV. Fig. 4 depicts the recorded instantaneous voltages.

For better visibility only a single phase, closely after CB opening is presented in the extended view (Fig. 4b). As one can observe in Fig. 4b, the impact of the harmonics present in the supply voltage on breaking process is evident. It is however doubtful, whether in this particular case the recorded difference of 4 kV in peak TRV is meaningful.

7. LV test circuit

The single phase LV circuit presented in this section was analysed using both simulations and laboratory setup, which is presented in Fig. 5.
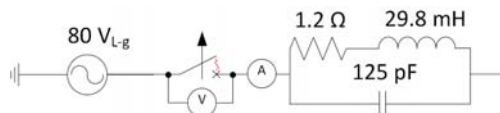
Fig. 5. Test LV circuit verified using simulations and experiments

It is composed of 29.8 mH air-core inductor, which was modelled as an equivalent linear RLC circuit that accounted for stray capacitance (with series damping resistor R = 600 Ω [1]), and wire resistance. The current was interrupted using typical three-phase electromechanical LV switch with double arc quenching chamber. Due to the fact that the considered circuit was a single phase arrangement only one pole of the switch was employed. When aiming at the good match of experiments and simulations, the representation of the electric arc forming between the CB electrodes during current interruption is of paramount importance. Hence, in this case the CB model based on methodology presented in chapter 2 was applied. It was represented by means of the variable resistor, whose resistance was accordingly controlled by the algorithm based on (5), (6) and (7). The algorithm was implemented using internal EMTP-ATP scripting language – MODELS. Values of the Cassie and Mayr equations coefficients as defined in (5) and (6) are listed in Table 2.

Table 2. Components data of the simplified HV test system [8]

τ_M	τ_C	U_0	P
μs		V	W
0.95	2	53.95	78

The model of source (i.e. network equivalent) was essentially determined by the laboratory setup. The circuit was powered by the controlled, single phase voltage source (type: Kikusui PCR1000LA), that could provide any user-defined waveform (e.g. harmonic spectrum) at its output. This device, except for continuous output voltage control, features a very low self-impedance. Hence, the network equivalent was modelled as an ideal voltage source with the harmonic spectrum as indicated in Table 3 (maximum permissible levels for individual harmonics distortion in the supply voltage [24]). Similar experiment was performed in [33].

Table 3. Individual harmonic content in supply voltage for LV test system (based on [24])

Harmonic Order	Relative Voltage	Harmonic Order	Relative Voltage
2, 17	2.0 %	9, 19 ,23, 25	1.5 %
3, 7	5.0 %	11	3.5 %
4	1.0 %	13	3.0 %
5	6.0 %	15, 21	0.5 %
7	5.0 %		

Other harmonics content (up to the 25th) were below 0.5% (set zero in simulation) [24]. The corresponding THD equals to 11.2%, therefore the selected harmonic spectrum could be considered as short-term effect [25, 26]. The nominal phase-to-ground RMS voltage (50 Hz component) accounted for 80 V. The resulting waveform is presented in Fig. 6.
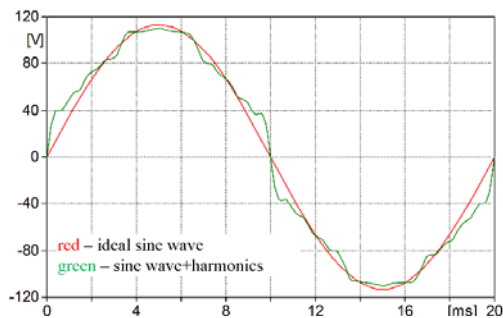
Fig. 6. Supply voltage (only single phase displayed) applied in experimental LV setup

7.2. Simulation and measurement results

This section presents the results obtained during the laboratory experiments conducted on setup, which is depicted in Fig. 5. The traces of current and TRV, recorded during measurements are depicted in Fig. 7.
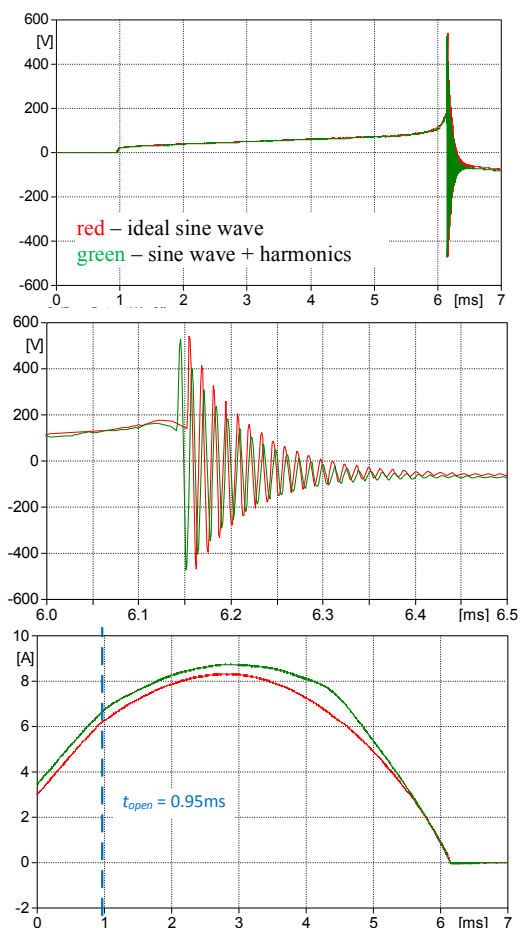
Fig. 7. Measured (experimental) waveforms for ideal supply voltage and supply voltage including harmonics; (a) TRV measured between contacts of CB, (b) TRV extended view, (c) interrupted current

The laboratory experiment was replicated by means of simulations that were carried out using EMPT-ATP. The simulated voltage and current waveforms are exhibited in Fig. 8.
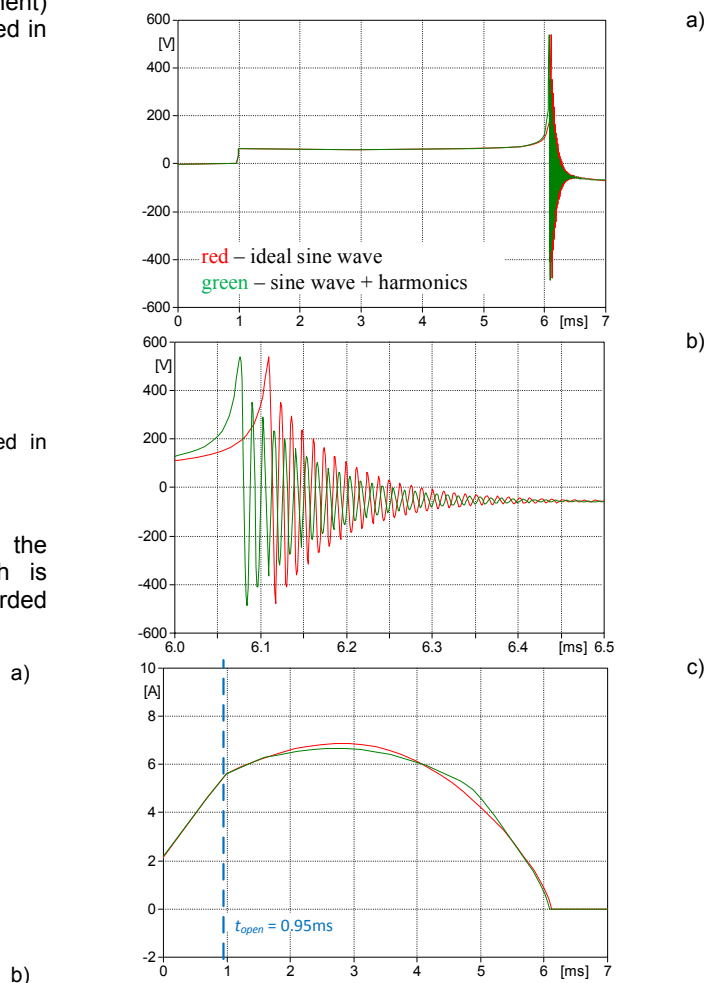
Fig. 8. Simulated waveforms for ideal supply voltage and supply voltage including harmonics; (a) TRV measured between contacts of CB, (b) TRV extended view, (c) interrupted current

Table 4 summarizes the results for this particular setup. It presents the peak TRV values and arcing times for all scenarios analysed in laboratory and by means of numerical simulations.

Table 4. Comparison of measurement and simulation results

Study on	Voltage supply type	TRV_{max}	t_{arc}
		V	ms
Simulations	Ideal source	540.2	5.164
	Source with harmonic	537.5	5.129
Measurements	Ideal source	541.4	5.142
	Source with harmonic	529.3	5.131

The experimental results of current interruption in the given circuit exhibited yet another confirmation of the impact of harmonics presence in the supply voltage on the current breaking process. This impact is reflected firstly in the peak value of TRV which appears between the switch contacts. Secondly, as it is displayed in Fig. 7, the breaking process is lowered by presence of harmonics (i.e. the arcing time is affected). Table 4 shows that in case of ideal sinusoidal voltage supply, the peak TRV is higher by 12 V and the

arcing time is 11 µs longer, than in situation when the voltage contains significant amount of harmonics. The harmonics did not influenced the oscillations appearing after the switch contacts separation.

The replication of experimental setup by means of simulation, also confirms the impact of presence of harmonics in the supply voltage both on peak TRV and arcing times. In case of simulation (Fig. 8), harmonics in voltage resulted as well in shorter arcing time (by 33.1 µs), and slightly lower higher peak value of the TRV (by 2.7 V). It is worth noting, that the simulated quantitative and qualitative results show satisfactory level of convergence. The arcing times are nearly the same and the maximum error (between simulations and experiments) in peak TRV is as high as 1.52%, which complies with safety factor 1.15 proposed in [2]. Comparison of measurement and simulation results obtained from analysis performed in considered LV circuit is presented in Table 4.

8. Impact of individual harmonics on switching overvoltages

The investigation of individual harmonics influence on the switching may indicate certain dependencies between harmonic order and the resulting TRV and arcing time. The circuit described in Chapter 5 was used for results preparation. In each case the harmonic content was the same (regardless of harmonic order) and it was set arbitrarily at 6% as a maximum value reported in [24].
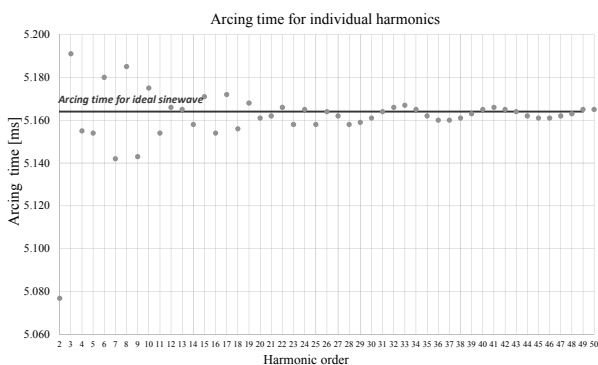
Fig. 9. Simulation results for individual harmonics impact verification on arcing time, with 6% content for each harmonic
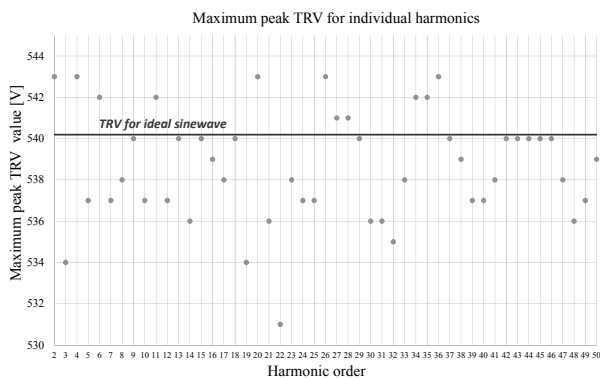
Fig. 10. Simulation results for individual harmonics impact verification on the TRV peak value, with 6% content for each harmonic

The results of investigation of individual harmonics are discussed in this chapter. For easy interpretation the results are shown in a graphical form. Relevant charts are depicted in Fig. 9 and Fig 10. The clear trend is visible especially for the arcing time Fig. 9. Its value converges to the arcing time

recorded for a purely sinusoidal supply. Also, the highest deviation from this value is visible for low order harmonics. This essentially means that higher the harmonic order, lower its impact on the switching process duration. Hence, based on the obtained results it could be stated that the relevance of high frequency components presence in the supply voltage has low impact on the arcing time. One can also observe that the TRV peak value can be also slightly influenced by the individual harmonics (regardless of its order) presence in the supply voltage.

9. Conclusions

As defined by CIGRE and IEC standards, the frequency of slow-front transients range from 50 Hz to 20 kHz, whereas e.g. for 60 Hz the 50th harmonic amounts to 3 kHz. Therefore, it was fair to assume that the harmonic contamination of supply voltage may affect the transient response, especially during current interruption, where expected frequency range of generated transient may overlap with the harmonic spectrum of the system voltage. This impact was evidently confirmed both by laboratory experiments and EMTP-ATP simulations.

In case of the HV system model, which was developed according to state-of-the-art methodology, the recorded peak value of TRV differs, depending on the harmonic spectrum of the supply voltage. In this case the presence of harmonics in the supply voltage slightly decreased the amplitudes of TRV. Nonetheless for given circuit conditions and harmonic content the difference of both results (with and without harmonics in voltage) is negligible. However, it is likely to assume that if the harmonic content changes, the peak TRV may follow.

The results obtained during experiments and simulations of LV test circuit confirmed the outcome of HV system simulations. However, the slight differences between experiments and simulation of LV circuit are at the acceptable level with error in recorded TRV as high as 1.51%. The alter in TRV peak (also in case of HV system) seems to partially origins from how it is measured (it is potential difference between load side and source side of the interrupter). However, the main reason for the change in arcing times is the harmonics contamination of the supply voltage. It is also noteworthy that due to inductive load, the resulting total harmonic distortion in current (THDi = 2.47%) was much lower than in voltage (THDv = 11.2%). Hence, currents being interrupted in case of ideal voltage supply and supply with harmonics, were nearly the same. The investigation of individual harmonics impact on the TRV and the arcing time has shown an interesting trend in arcing time recorded in presence of higher order harmonics. It is visible that higher the harmonic order lower its impact on arcing time compared to sinusoidal supply. Such trend was not visible for the TRV value, however it was also slightly influenced regardless of the harmonic order present in the supply voltage.

Finally, based on performed measurements and simulations, it can be clearly stated that the presence of harmonics in the supply voltage impacts the resulting TRV and arcing time during switching transient studies. This impact seems to be negligible, therefore it can be concluded that the standardized approach of modelling recommended by e.g. IEC and IEEE provides sufficient accuracy and the harmonics in supply voltage can be disregarded for switching transient studies.

Authors. Tomasz Chmielewski, PhD, ABB Corporate Research Center, Starowiślna 13 A Str., 31-038 Krakow, Poland, e-mail: tomasz.chmielewski@pl.abb.com

Piotr Oramus, PhD, ABB Corporate Research Center, Starowiślna 13 A Str., 31-038 Krakow, Poland,
e-mail: piotr.oramus@pl.abb.com
Tomasz Kuczek, PhD, ABB Corporate Research Center, Starowiślna 13 A Str., 31-038 Krakow, Poland,
e-mail: tomasz.kuczek@pl.abb.com

REFERENCES

[1] IEC 60071-4:2004: Insulation co-ordination – Part 4: Computational guide to insulation co-ordination and modelling of electrical networks
[2] IEC 60071-2: 2004. Insulation co-ordination – Part 2: Application Guide
[3] IEEE Guide for the Application of Insulation Coordination. IEEE Std 1313.2-1999
[4] IEEE Recommended Practice for Industrial and Commercial Power Systems Analysis, IEEE Std 399-1997
[5] IEEE Recommended Practice for Overvoltage and Insulation Co-ordination of Transmission Systems at 1000 kV AC and Above, IEEE Std 1862™-2014
[6] Application Guide for Transient Recovery Voltage for AC High-Voltage Circuit Breakers, IEEE Std C37.011™-2005:
[7] CIGRE Working Group 02 (SC 33), "Guidelines for Representation of Network Elements when Calculating Transients," CIGRE Brochure 39, 1990
[8] Modeling and Analysis of System Transients Modeling and Analysis of System Transients Using Digital Programs, IEEE working group 15.08.09. 2013
[9] The calculation of switching surges – III. Transmission line representation for energization and re-energization studies with complex feeding networks" – CIGRE study committee 13 – Electra Nr 62
[10] Kuczek T., Florkowski M., Piasecki W.: Analyses of vacuum circuit breaker switching transients in medium voltage networks with respect to LC filters of solar converters, International Conference on HV Engineering and Application, Poznań, 2014
[11] Oramus P., Smugała D., Zydroń P.: Modeling of specific harmonics source in EMTP-ATP, Przegląd Elektrotechniczny R. 89, No. 8/2013, pp. 20-324, 2013
[12] Sowa K., Baszyński M., Piróg S.: Jednofazowy energetyczny filtr aktywny z zasobnikiem energii do kompensacji wahań mocy czynnej w linii zasilającej, Przegląd Elektrotechniczny, vol. 93, no. 3, pp. 260-266, 2017
[13] Kowalak R., Czapp S., Dobrzyński K., Klucznik J., Lubośny Z.: Harmonics produced by traction substations – computer modelling and experimental verification, Przegląd Elektrotechniczny, R. 93, nr 6/2017, pp. 13-18, 2017
[14] Kandyba, A.: Modelling of gliding arc in non-thermal plasma reactors, Przegląd Elektrotechniczny, R. 89, Nr 2a/2013, p 51-54, 2013
[15] Chmielak, W.: ATP/EMTP modelling and simulation of current interruptions by vacuum current breaker in respect of post-arc phenomena, Przegląd Elektrotechniczny, R. 86, Nr 12/2017, p. 208-211, 2010
[16] Budzisz J., Wróblewski Z.: Modeling of switching effects in capacitive circuit with a vacuum switch and varistor surge protection, Przegląd Elektrotechniczny, R. 88, Nr 5a/2012, pp. 284-289, 2012
[17] Annakkage, U.D.; Nair, N.K.C.; Liang, Y.; Gole, A.M.; Dinavahi, V.; Gustavsen, B.; Noda, T.; Ghasemi, Hassan; Monti, A.; Matar, M.; Iravani, R.; Martinez, J.A., "Dynamic System Equivalents: A Survey of Available Techniques," Power Delivery, IEEE Transactions on , vol.27, no.1, pp.411,420, Jan. 2012
[18] Dawidowski P., Sowa K., Stosur M., Szewczyk M., Balcerek P.: „Reduction of THD by switching frequency optimization in three-level NPC inverter", Przegląd Elektrotechniczny,R. 90 nr 8/2014, pp. 18-21, 2014
[19] Yuefeng Liang; Xi Lin; Gole, A.M.; Ming Yu, "Improved Coherency-Based Wide-Band Equivalents for Real-Time Digital Simulators," Power Systems, IEEE Transactions on , vol.26, no.3, pp.1410,1417, Aug. 2011
[20] Matar, M.; Iravani, R., "A Modified Multiport Two-Layer Network Equivalent for the Analysis of Electromagnetic Transients," Power Delivery, IEEE Transactions on , vol.25, no.1, pp.434,441, Jan. 2010
[21] Shun Liang, Qiaohui Hu, Wei-Jen Lee: A Survey of Harmonic Emissions of a Commercially Operated Wind Farm, IEEE Transactions on Industry Applications, VOL. 48, NO. 3, MAY/JUNE 2012, pp. 1115-1123
[22] M.J. Ortega, J.C. Hernández, O.G. García: Measurement and assessment of power quality characteristics for photovoltaic systems: Harmonics, flicker, unbalance, and slow voltage variations, Electric Power Systems Research, March 2013, pp. 23-35
[23] Babak Badrzadeh, Manoj Gupta: Practical Experiences and Mitigation Methods of Harmonics in Wind Power Plants, IEEE Transactions on Industry Applications, VOL. 49, NO. 5, September/October 2013, pp. 2279-2289
[24] EN50160, "Voltage characteristics of electricity supplied by public electricity networks", 2010
[25] IEEE Draft Guide for Applying Harmonic Limits on Power Systems," IEEE P519.1/D12, July 2012 , vol., no., pp.1,124, Feb. 26 2015
[26] IEC 61000-2-2, EMC Part 2-2: Environment Compatibility levels for low frequency conducted disturbances and signalling in public low-voltage power supply systems, 2002
[27] IEC 61000-2-1, EMC Part 2-1: Description of the environment — Electromagnetic environment for low-frequency conducted disturbances and signalling in public power supply systems, 1990
[28] Electrical Transient Interaction Between Transformers and the Power System, Part 1: Expertise, CIGRE Joint Working Group A2/C4.39, ISBN: 978-2-85873272-2, 2014
[29] IEEE Guide To Describe The Occurrence and Mitigation Of Switching Transients Induced By Transformer Switching Device and System Interaction, IEEE C57.142, September, 2010
[30] CIGRE WG 13.01, State of the art of circuit- breaker modelling, 1998
[31] Chmielewski T., Oramus P., Florkowski M.: Modelowanie łuku elektrycznego w analizach przepięć łączeniowych podczas przerywania prądu przy użyciu niskonapięciowych przekaźników elektromechanicznych, Przegląd Elektrotechniczny (ISSN 0033-2097) No. 2/2016, pp. 202-206, 2016
[32] An improved circuit-breaker model in models language for ATP-EMTP code, IPST '99 - International Conferences on Power Systems Transients, Budapest - Hungary, pp. 493-498, June 20-24, 1999
[33] Otomański P., Wiczyński G.: Wykorzystanie programowalnego źródła napięcia przemiennego do generacji wyższych harmonicznych w badaniach jakości energii elektrycznej, Przegląd Elektrotechniczny nr 8/2015, R. 91, pp. 38-41, 2015